Pergamon

Int. J. Solids Structures Vol. 34, No. 20, pp. 2595–2609, 1997

0020–7683/97 $17.00 + .00

PII: S0020–7683(96)00157–6

THE USE OF FINITE EXTENSION STRAIN ENERGY RELEASE RATES IN FRACTURE OF INTERFACIAL CRACKS

C. T. SUN and W. QIAN
School of Aeronautics and Astronautics, Purdue University, West Lafayette, IN 47907-1282, U.S.A.

(*Received* 24 *October* 1995; *in revised form* 15 *July* 1996)

Abstract—The existing solutions for interfacial cracks in bimaterial media obtained from the contact model and oscillatory model were compared. The oscillatory near tip stress field was found to agree very well with that of the contact model except for the extremely small contact zone. Using the oscillatory solution, Mode I and Mode II "strain energy release rates" for finite crack extensions were obtained in terms of the stress intensity factors and the assumed crack extension Δa. Finite elements in conjunction with the crack closure method were used to calculate these "strain energy release rates" from which accurate stress intensity factors were obtained. An alternative and efficient method based on crack surface displacement ratio was also introduced to obtain stress intensity factors. Non-oscillatory (Δa-independent) Mode I and Mode II "strain energy release rates" were proposed to provide an alternate measure of fracture mode mixity or to be used as a fracture criterion for interfacial cracks. © 1997 Elsevier Science Ltd

1. INTRODUCTION

The problem of interfacial crack between two dissimilar isotropic materials was first investigated by Williams (1959) who performed an asymptotic analysis of the elastic field at the tip of an open crack and found that the stress field possesses an oscillatory character of the type $r^{-1/2+i\varepsilon}$, where r is the radial distance from the crack tip and ε is the bimaterial constant. England (1965) showed that this kind of oscillation is physically inadmissible since it predicts that the upper and lower surfaces of the crack should wrinkle and overlap near the end of the crack. The zone over which the solution predicts overlapping of materials is very small in comparison with the length of crack for tensile loading. However, it could be large for shear loading (Comninou, 1978). Rice and Sih (1965) applied the complex variable technique of Muskhelishvili combined with eigenfunction expansion to explicitly obtain the expression of stress components in the vicinity of an interfacial crack tip.

In the late seventies, Comninou (1977, 1978, 1979) proposed the contact zone model which recognized the unilateral nature of the crack problem. Because of the extremely small size of the contact zone near the tip, Comninou's solutions from a direct numerical method for a singular integral equation is only good for some extreme mismatches in elastic constants. Gautsen and Dundurs (1987, 1988) showed the integral equation formulated by Comninou could be solved exactly. They noted that the value of the stress intensity factor they obtained agreed well with the numerical result given by Comninou and Schmueser (1979) for the crack tip with large contact zone, while the agreement was poor for the crack tip with small contact zone. However, their solution procedure is exceedingly complicated. Subsequently, Gautsen (1993) obtained simple asymptotic approximations to the quantities of physical interest such as the size of contact zone and the tractions in the plane of the crack.

Although the Comninou contact zone model may provide the only valid mathematical solution of the true interface crack in the context of LEFM, it is impractical to search for fracture design parameters characterizing the failure on the basis of the contact zone model because of its extremely small contact zone size. Moreover, the elastic interfacial crack solutions that allow interpenetration of the crack surfaces near the crack tip do nevertheless describe near-tip state when the size of the zone is much smaller than the crack length. As

stated by Rice (1988), the actual field in the small scale nonlinear or contact zone case is uniquely characterized by a complex elastic stress intensity factor, even though the elastic solution is not correct in that zone.

In the present study, existing solutions for bimaterial interfacial cracks based on both oscillatory model and contact model are compared. The near tip stresses and the sizes of the contact zone and stress oscillation zone are investigated. Alternative expressions for the interfacial crack mode mixity are introduced. Due to the oscillatory nature of the stress and displacement fields at the crack tip, the Mode I and Mode II strain energy release rates do not exist. However, the crack closure integrals can be evaluated for a finite crack extension from which the stress intensity factors can be derived. Besides, the ratio of stress intensity factors can also be evaluated alternatively from the crack surface displacement ratio. With these approaches, the finite element method can be used efficiently to calculate stress intensity factors for general geometries and loading. Numerical results are presented to show the accuracy of these techniques.

2. STRESS INTENSITY FACTOR AND NEAR TIP STRESS FIELD

There are many definitions of stress intensity factors depending on the solution forms selected for the interfacial crack problem (e.g. Rice and Sih, 1965; Malysev and Salganik, 1965; Hutchinson *et al.*, 1987; Sun and Jih, 1987). Most of these definitions differ by either a phase factor or a constant.

Hutchinson *et al.* (1987) introduced a complex $K = K_I + iK_{II}$ in such a way that, along the interface ahead of the crack tip, stresses are given by

$$(\sigma_{yy} + i\sigma_{xy})_{\theta=0} = K_h r^{i\varepsilon}/\sqrt{2\pi r} \tag{1}$$

where

$$\varepsilon = \frac{1}{2\pi}\ln\left[\left(\frac{\kappa_1}{\mu_1}+\frac{1}{\mu_2}\right)\Big/\left(\frac{\kappa_2}{\mu_2}+\frac{1}{\mu_1}\right)\right]. \tag{2}$$

For the interface crack of length $2a$ subject to remotely uniform stresses σ_{yy}^{∞} and σ_{xy}^{∞}, the complex stress intensity factor by Hutchinson *et al.* (1987) is

$$K_h = (\sigma_{yy}^{\infty} + i\sigma_{xy}^{\infty})(1+2i\varepsilon)(2a)^{-i\varepsilon}\sqrt{\pi a}. \tag{3}$$

This stress intensity factor is related to the complex stress intensity factor K_r proposed by Rice and Sih (1965) as

$$K_r = K_h/\sqrt{\pi}\cosh(\pi\varepsilon). \tag{4}$$

Both K_h and K_r contain a crack length-related phase term $(2a)^{-i\varepsilon}$ giving rise to a complex dimension. Consequently, the stress intensity factor becomes a function of the unit that measures the crack length.

Malysev *et al.* (1965) introduced the stress intensity factor by expressing the crack tip stresses as

$$(\sigma_{yy} + i\sigma_{xy})_{\theta=0} = K_m(r/2a)^{i\varepsilon}/\sqrt{2\pi r}. \tag{5}$$

For the interface crack of length $2a$ subject to remotely uniform stresses σ_{yy}^{∞} and σ_{xy}^{∞},

$$K_m = (\sigma_{yy}^{\infty} + i\sigma_{xy}^{\infty})(1+2i\varepsilon)\sqrt{\pi a}. \tag{6}$$

The complex stress intensity factor K_s introduced by Sun and Jih (1987) is related to K_m as

$$K_s = K_m/\cosh(\pi\varepsilon). \tag{7}$$

The relationship between K_h and K_s is

$$K_h = K_s(2a)^{-i\varepsilon}\cosh(\pi\varepsilon). \tag{8}$$

Both K_m and K_s remove the ambiguity of dimension by excluding the term $(2a)^{-i\varepsilon}$ and both have the same dimension as classical stress intensity factor. However, the fact that $(2a)^{-i\varepsilon}$ is removed from the definition of the stress intensity factor and therefore has to be included in the angular distribution function of the field solution avoids the crack length unit effect in the stress intensity factor but leads to a situation where cracks with the same stress intensity factor but different lengths have different near-tip fields. Nevertheless, all above definitions of stress intensity factor are acceptable as far as the near-tip state is concerned. In addition, these definitions are related to each other. Henceforth, K_s will be adopted and replaced by K for simplicity in the following sections.

In order to confirm the validity of the elastic oscillatory solution for the interfacial crack in the context of small scale contact zone concept, we consider the near-tip stress fields for a two-dimensional infinite medium with a center crack of size $2a$ subject to remotely uniform tensile stress σ_{yy}^{∞} given by Sih and Rice (1965) from the oscillatory model by Gautsen and Dundurs (1987) from the contact model. The asymptotic crack tip stresses along the interface ahead of the crack tip from the oscillatory solution are

$$\sigma_{yy} = \frac{\sigma_{yy}^{\infty}}{\sqrt{2x/a}}\left[\cos\left(\varepsilon\ln\frac{x}{2a}\right) - 2\varepsilon\sin\left(\varepsilon\ln\frac{x}{2a}\right)\right] \tag{9}$$

$$\sigma_{xy} = \frac{\sigma_{xy}^{\infty}}{\sqrt{2x/a}}\left[\sin\left(\varepsilon\ln\frac{x}{2a}\right) + 2\varepsilon\cos\left(\varepsilon\ln\frac{x}{2a}\right)\right] \tag{10}$$

where

$$\kappa_j = \begin{cases} 3-4\nu_j & \text{for plane strain} \\ (3-\nu_j)/(1+\nu_j) & \text{for plane stress} \end{cases}.$$

Here, μ is shear modulus, ν is Poisson's ratio and subscripts 1 and 2 denote upper and lower materials, respectively.

The exact solution from the contact model was given by Gautsen and Dundurs (1987) as

$$\sigma_{yy} = \frac{\sigma_{yy}^{\infty}}{t}(1+\beta_0^2/\pi^2)^{1/2}\sin w_2 + \frac{\hat{s}_3(w)-\hat{s}_3(-w)}{t} \tag{11}$$

$$\sigma_{xy} = \frac{\sigma_{xy}^{\infty}}{t}(1+\beta_0^2/\pi^2)^{1/2}\cos w_2 + \hat{s}_1(w)+\hat{s}_1(-w) \tag{12}$$

where

$$\beta_0 = \ln\left(\frac{1+\beta}{1-\beta}\right), \quad t = \sqrt{\frac{x}{a}\left(2+\frac{x}{a}\right)}$$

and

$$\beta = \frac{\mu_2(\kappa_1 - 1) - \mu_1(\kappa_2 - 1)}{\mu_2(\kappa_1 + 1) + \mu_1(\kappa_2 + 1)} \tag{13}$$

is one of the two Dundurs parameters. All other parameters in (11) and (12) can be found in the Appendix. Note that β is also related to ε as $\varepsilon = (1/2\pi)\ln(1+\beta)/(1-\beta)$.

The log–log plot of the normal and shear stresses ahead of the crack tip in the remote tension field from the contact model and the oscillatory model are shown in Fig. 1 for $\beta = 0.2$ and $\beta = 0.5$, where $\beta = 0.5$ stands for the largest mismatch of elastic constants. From the plots in Fig. 1, it is evident that solutions from both models agree extremely well beyond $x/a = 10^{-4}$, except for the normal stress associated with $\beta = 0.5$. For this case, the normal stresses from the two models agree up to $x/a = r_0 \approx 2.51 \cdot 10^{-4}$. This value turns out to be the size of the oscillation (or overlap) zone for the crack-tip normal stress.

Let r_0 and r_0^* denote the oscillation zones of normal stress and shear stress, respectively. Without loss of generality, we assume $\varepsilon > 0$. The oscillation zone size r_0 for the normal stress σ_{yy} can be determined by finding the largest value of x at which $\mathrm{d}\sigma_{yy}/\mathrm{d}x = 0$. We obtain

$$r_0 = 2a\exp\left(-\frac{\pi}{2\varepsilon}\right). \tag{14}$$

It is not difficult to show that r_0 is the same as the overlap zone in which the crack surfaces interpenetrate.

Similarly, by letting $\mathrm{d}\sigma_{xy}/\mathrm{d}x = 0$ along with eqn (1), we find the oscillation zone r_0^* for the shear stress as

$$r_0^* = 2a\exp\left(-\frac{\pi}{\varepsilon}\right). \tag{15}$$

From eqns (14) and (15) we can see that the size of the oscillation zone for the shear stress

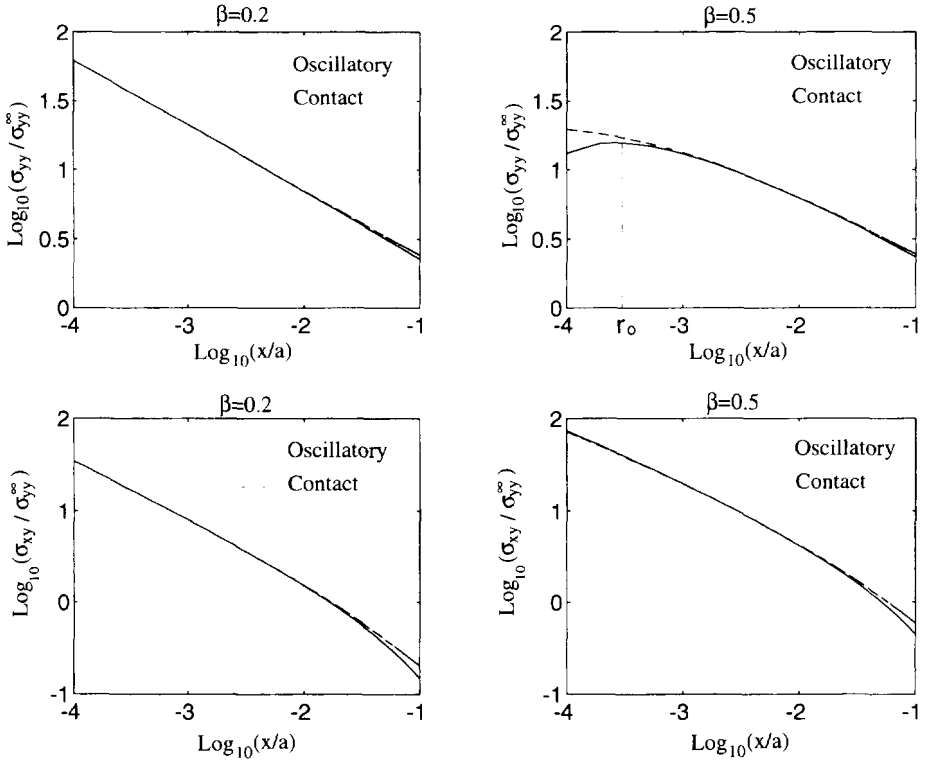

Fig. 1. Comparison of normal and shear stresses ahead of the crack tip obtained from the oscillatory model and the contact model.

Table 1. The comparison of oscillation zone and contact zone for different $\sigma_{xy}^{\infty}/\sigma_{yy}^{\infty}$ ratios and $\nu_1 = \nu_2 = 0.3$

	$\sigma_{xy}^{\infty}/\sigma_{yy}^{\infty} = 0.0$		$\sigma_{xy}^{\infty}/\sigma_{yy}^{\infty} = 0.5$		$\sigma_{xy}^{\infty}/\sigma_{yy}^{\infty} = 1$	
	$r_0/2a$	$r_c/2a$	$r_0/2a$	$r_c/2a$	$r_0/2a$	$r_c/2a$
E_1/E_2	Overlap	Contact	Overlap	Contact	Overlap	Contact
5	1.923×10^{-9}	1.057×10^{-9}	8.820×10^{-7}	4.847×10^{-7}	6.201×10^{-5}	3.408×10^{-5}
10	1.065×10^{-7}	5.899×10^{-8}	1.494×10^{-5}	8.273×10^{-6}	4.615×10^{-4}	2.556×10^{-4}
100	2.032×10^{-6}	1.137×10^{-6}	1.194×10^{-4}	6.682×10^{-5}	2.016×10^{-3}	1.128×10^{-3}

is much smaller than that for the normal stress. This feature is noted in Fig. 1. Specifically, for $\beta = 0.5$, we have $r_0/a = 2.51 \cdot 10^{-4}$, $r_0^*/a = 3.15 \cdot 10^{-8}$, while for $\beta = 0.2$, $r_0/a = 5.34 \cdot 10^{-11}$ and $r_0^*/a = 1.44 \cdot 10^{-21}$. Thus, except for extreme mismatch cases, the oscillation zone is extremely small as compared with the crack size. In other words, the near-tip solutions from the oscillatory model and the contact model are practically identical except for an extremely small region near the crack tip. This finding also justifies matching asymptotic expressions of nonlinear models for the neartip zone (Bui, 1994).

3. OSCILLATION ZONE AND CONTACT ZONE

In general, the oscillation zone from the oscillatory model and the contact zone from the contact model are quite different. For illustration, consider an infinite bimaterial medium with a center interfacial crack $2a$ subject to remotely uniform normal and shear stresses. Let

$$\sigma_{yy}^{\infty} + i\sigma_{xy}^{\infty} = Te^{i\psi} \tag{16}$$

where the phase angle is given by

$$\psi = \tan^{-1}\left(\frac{\sigma_{xy}^{\infty}}{\sigma_{yy}^{\infty}}\right).$$

Rice (1988) estimated the contact zone by the oscillation zone r_0 from the oscillatory solutions as

$$r_0 = 2a\exp\left[-\frac{1}{\varepsilon}\left(\frac{\pi}{2} + \psi\right)\right]. \tag{17}$$

It is noted that the contact zone size for a given bimaterial medium estimated according to eqn (17) is solely dependent on ψ. The contact zone r_c from the contact model was given by Gautsen (1993). Both results are shown in Table 1 for three different loading conditions. It is noted that the Rice's estimation r_0 is approximately twice the true contact zone r_c. Nevertheless, the value r_0 provides a convenient estimate of the contact zone.

It is necessary that restrictions be imposed on the contact zone size in order that the small scale contact concept may be applied. From Sun and Jih (1987), the near-tip relative displacement along the crack surfaces is

$$\Delta u_y = u_y(r,\pi) - u_y(r,-\pi) = \frac{\sqrt{2r}}{4(1+4\varepsilon^2)\sqrt{\pi}}\left[\frac{\kappa_1+1}{\mu_1} + \frac{\kappa_2+1}{\mu_2}\right]\{K_I H_1 - K_{II} H_2\} \tag{18}$$

$$\Delta u_x = u_x(r,\pi) - u_x(r,-\pi) = \frac{\sqrt{2r}}{4(1+4\varepsilon^2)\sqrt{\pi}}\left[\frac{\kappa_1+1}{\mu_1} + \frac{\kappa_2+1}{\mu_2}\right]\{K_I H_2 + K_{II} H_1\} \tag{19}$$

where

$$H_1 = \left[\cos\left(\varepsilon \ln\left(\frac{r}{2a}\right)\right) + 2\varepsilon \sin\left(\varepsilon \ln\left(\frac{r}{2a}\right)\right)\right] \tag{20}$$

$$H_2 = \left[\sin\left(\varepsilon \ln\left(\frac{r}{2a}\right)\right) - 2\varepsilon \cos\left(\varepsilon \ln\left(\frac{r}{2a}\right)\right)\right]. \tag{21}$$

We estimate the contact zone size by adopting r_0 which is the largest r at which the relative normal displacement given by (18) vanishes, i.e.

$$K_I H_1 - K_{II} H_2 = 0. \tag{22}$$

Equation (22) together with (20) and (21) yields

$$r_0 = 2a \exp\left[\frac{1}{\varepsilon}\left(\tan^{-1}\left(\frac{K_I + 2\varepsilon \cdot K_{II}}{K_{II} - 2\varepsilon \cdot K_I}\right) - \pi\right)\right]. \tag{23}$$

The above expression being in terms of K_I and K_{II} is more general than that of (17).

For an infinite bimaterial medium with remote loading, we have

$$K_I = \sqrt{\pi a}[\sigma_{yy}^{\infty} - 2\varepsilon\sigma_{xy}^{\infty}]/\cosh(\pi\varepsilon) \tag{24}$$

$$K_{II} = \sqrt{\pi a}[\sigma_{xy}^{\infty} + 2\varepsilon\sigma_{yy}^{\infty}]/\cosh(\pi\varepsilon). \tag{25}$$

Substitution of eqns (24) and (25) into eqn (23) leads to eqn (17) obtained by Rice (1988).

Redefining the phase angle ψ as

$$\tan\psi = \frac{K_{II}}{K_I} \tag{26}$$

we can rewrite eqn (23) as

$$\frac{r_0}{2a} = \exp\left[\frac{1}{\varepsilon}\left(\tan^{-1}\left(\frac{1 + 2\varepsilon\tan\psi}{\tan\psi - 2\varepsilon}\right) - \pi\right)\right]. \tag{27}$$

The value of $r_0/2a$ has to be less than a certain value where the small scale contact concept can be applied. To ensure that the crack tip state is K-dominated, Rice (1988) suggested that $r_0/2a \leqslant 0.01$, or equivalently,

$$\frac{1 + 2\varepsilon\tan\psi}{\tan\psi - 2\varepsilon} \leqslant \tan(\varepsilon \ln 0.01). \tag{28}$$

4. CALCULATION OF STRESS INTENSITY FACTORS USING FINITE ELEMENT ANALYSIS

Classical methods for solving the stress intensity factor for the interfacial crack problems are limited to a few special cases due to the inherent mathematical difficulties. Numerical methods such as the finite element method are needed to calculate the stress intensity factors for interface cracks in bodies of finite dimensions under general loading conditions. Because of the extremely small oscillation (or contact) zone near the crack tip, the use of regular finite elements is obviously not practical. Lin and Mar (1976) employed a special bimaterial crack element to model the crack tip region. This crack element was derived based on the interfacial crack tip stress field and the hybrid formulation. Matos *et al.* (1988) proposed a method for calculating the stress intensity factor based on the evaluation of the

J-integral, and individual stress intensities can be obtained from further calculation of J perturbed by small increments of the stress intensity factors. In the following, two efficient methods are introduced to obtain the stress intensity factors from finite element analysis.

4.1. *Energy method*

A finite element-based crack closure method has been shown to be very efficient in calculating the strain energy release rate for cracks in homogeneous media (Rybicki and Kanninen, 1977; Raju *et al.*, 1988; Jih and Sun, 1990). The stress intensity factor can be derived from the strain energy release rate using the relation between these two quantities. For bimaterial interfacial cracks, however, the strain energy release rates for Mode I and Mode II do not exist due to their oscillatory nature (Sun and Jih, 1987; Raju *et al.*, 1988). Thus, no converged strain energy release rates G_{I} and G_{II} can be calculated using finite element method with the crack closure method.

If we allow a finite crack extension Δa (and thus a finite crack closure length) in Irwin's crack closure integrals, i.e.

$$\hat{G}_{\mathrm{I}} = \frac{1}{2\Delta a}\int_0^{\Delta a} \sigma_{yy}(x,0)\Delta u_y(\Delta a - x,\pi)\,\mathrm{d}x \tag{29}$$

$$\hat{G}_{\mathrm{II}} = \frac{1}{2\Delta a}\int_0^{\Delta a} \sigma_{xy}(x,0)\Delta u_x(\Delta a - x,\pi)\,\mathrm{d}x \tag{30}$$

then, these integrals can be evaluated without ambiguity. Indeed, Sun and Jih (1987) obtained these finite extension strain energy released rates as

$$\hat{G}_{\mathrm{I}} = \tfrac{1}{2}G + C[A_{\mathrm{R}}(K_{\mathrm{I}}^2 - K_{\mathrm{II}}^2) - 2A_{\mathrm{I}}K_{\mathrm{I}}K_{\mathrm{II}}] \tag{31}$$

$$\hat{G}_{\mathrm{II}} = \tfrac{1}{2}G - C[A_{\mathrm{R}}(K_{\mathrm{I}}^2 - K_{\mathrm{II}}^2) - 2A_{\mathrm{I}}K_{\mathrm{I}}K_{\mathrm{II}}] \tag{32}$$

where

$$G = D(K_{\mathrm{I}}^2 + K_{\mathrm{II}}^2) \tag{33}$$

is the total strain energy release rate and

$$A_{\mathrm{R}} = Re(A)$$

$$A_{\mathrm{I}} = -Im(A)$$

$$A = B\left[\frac{\Delta a}{4a}\right]^{-2i\varepsilon}$$

$$B = \frac{\sqrt{\pi}}{2}\left[\frac{1}{2}+i\varepsilon\right]\Gamma\left[\frac{1}{2}-i\varepsilon\right]/\Gamma[1-i\varepsilon]$$

$$C = \frac{\cosh(\pi\varepsilon)}{4(1+4\varepsilon^2)\pi}\left[\frac{\kappa_1+1}{\mu_1}+\frac{\kappa_2+1}{\mu_2}\right]\left[1+\frac{\Delta a}{2a}\right]$$

$$D = \frac{1}{16}\left[\frac{\kappa_1+1}{\mu_1}+\frac{\kappa_2+1}{\mu_2}\right].$$

In the above quantities, Γ is the gamma function and $Re(\ )$ and $Im(\ )$ denote the real part and imaginary part of a complex quantity, respectively. By solving equations (31) and (32)

for K_I and K_{II}, and neglecting the negative solution for K_I, we obtain the stress intensity factors in terms of $\hat{G}_I$ and $\hat{G}_{II}$ as

$$K_I = \sqrt{\frac{4A_R S + 4A_I^2 \frac{G}{D} \pm \sqrt{\left(4A_R S + 4A_I^2 \frac{G}{D}\right)^2 - 16(A_R^2 + A_I^2)S^2}}{8(A_R^2 + A_I^2)}} \tag{34}$$

$$K_{II} = \frac{2A_R K_I^2 - S}{2A_I K_I} \tag{35}$$

where

$$S = \frac{\hat{G}_I - \hat{G}_{II}}{2C} + \frac{A_R G}{D}.$$

The relations in (34) and (35) indicate that, for one set of $\hat{G}_I$ and $\hat{G}_{II}$, we may have two sets of solution for K_I and K_{II}. However, there is only one set of K_I and K_{II} which is physically meaningful. We can extract the correct K_I and K_{II} guided by conditions on the crack surface displacements.

We assume that the Δa selected for calculating $\hat{G}_I$ and $\hat{G}_{II}$ satisfying $\Delta a > r_0$, where r_0 is the size of oscillation zone. Therefore, the relative normal crack surface displacement must be positive, while the sign of relative tangential crack surface displacement Δu_x can be determined easily from the finite element result. Hence, the displacement conditions for selecting the roots of K_I and K_{II} for interface cracks are

$$\Delta u_y(\Delta a) > 0 \quad \text{and} \quad sgn(\Delta u_x): \quad \text{determined by FEA.} \tag{36}$$

In other words, from eqns (18) and (19), the condition for selecting K_I and K_{II} are

$$K_I H_1 - K_{II} H_2 > 0, \quad sgn(K_I H_2 + K_{II} H_1) = sgn(\Delta u_x): \quad \text{determined by FEA.} \tag{37}$$

For $\varepsilon = 0$, there is only one pair of K_I and K_{II}.

4.2. *Displacement ratio method*

The stress intensity factors can also be obtained through their relations with the neartip displacements as given by eqns (18) and (19). As shown by Matos *et al.* (1988), the stress intensity factors obtained directly from these relations are not reliable. Indeed, depending on the location at which these crack surface displacements are taken, the stress intensity factors may vary appreciably. Matos *et al.* (1988) resorted to the use of the J integral to aid the selection of the location of crack surface displacements to produce the optimal result.

Recognizing that the individual crack surface displacements, Δu_x and Δu_y obtained from FEA may not be accurate, but the ratio $\Delta u_x/\Delta u_y$ seems to be more accurate, we propose that this ratio be used to determine the ratio K_{II}/K_I.

Using the eqns (18) and (19), the ratio of K_{II}/K_I can be expressed in terms of displacement ratio $\Delta u_y/\Delta' u_x$ as

$$\frac{K_{II}}{K_I} = \frac{H_1 - H_2 \times \Delta u_y/\Delta u_x}{H_2 + H_1 \times \Delta u_y/\Delta u_x}. \tag{38}$$

Individual stress intensity factors K_I and K_{II} can be obtained from eqns (33) and (38). It is easy to see that the displacement ratio method is more convenient to perform than the energy method.

5. MODE MIXITY

Due to the oscillatory singularity in the near tip stress field, K_I and K_{II} for interfacial cracks cannot be uniquely associated with Mode I and Mode II fracture as defined in homogeneous media. Nevertheless, K_I and K_{II} still represent two modes of fracture action and their relative amount of participation in fracture can be reflected by the mode mixity angle defined by

$$\psi_K = \tan^{-1}\left(\frac{Im(K)}{Re(K)}\right). \tag{39}$$

If we adopt a definition of stress intensity factor that includes the phase effect of crack length such as Hutchinson *et al.* (1987), the mode mixity ψ_K would be ambiguous due to the nature of oscillatory singularity of the interfacial crack. In order to define the mixed mode fracture toughness unambiguously, Rice (1988) suggested a definition of stress intensity factor of the classical type denoted by $K_I + iK_{II}$ which circumvented these difficulties, i.e.

$$K_I + iK_{II} = K_h \hat{r}^{i\varepsilon} \tag{40}$$

where $\hat{r}$ is chosen to be independent of the overall specimen size and specimen types. It is easy to see that $K_I + iK_{II}$ obtained at one $\hat{r}$ can be converted to those at a different $\hat{r}$. Hence, there are no restrictions in the selection of $\hat{r}$. It is readily seen that if $\hat{r}$ is chosen to be $2a$, then the definition of (40) becomes identical to that of Sun and Jih (1987) except for a real constant factor $\cosh \pi\varepsilon$ (see eqn (8)).

The mixed mode fracture condition can be given as

$$G(\psi_K) = G_c(\psi_K) \tag{41}$$

$$\psi_K = \tan^{-1}\left(\frac{K_{II}}{K_I}\right). \tag{42}$$

The above fracture criterion was suggested by Hutchinson (1990) for the case $\varepsilon = 0$ for which the mode mixity ψ_K can be unambiguously defined in terms of K_h. When $\varepsilon = 0$, G_I and G_{II} are well defined and the mode mixity can be also fully expressed in terms of the strain energy release rates as

$$\psi_G = \tan^{-1}\left(\frac{G_{II}}{G_I}\right). \tag{43}$$

However, the mode mixity cannot be expressed for bimaterial interface cracks in terms of the ratio of $\hat{G}_{II}$ and $\hat{G}_I$ due to their Δa dependency and their nonconvergent nature (as $\Delta a \to 0$). In view of the foregoing, we rewrite the finite extension strain energy release rates $\hat{G}_I$ and $\hat{G}_{II}$ in (31) and (32) as

$$\hat{G}_I = \frac{1}{2}G + \frac{C|B|G}{D}\left[\cos(\theta-\phi)\cos\left(2\varepsilon \ln\frac{\Delta a}{4a}\right) + \sin(\theta-\phi)\sin\left(2\varepsilon \ln\frac{\Delta a}{4a}\right)\right] \tag{44}$$

$$\hat{G}_{II} = \frac{1}{2}G - \frac{C|B|G}{D}\left[\cos(\theta-\phi)\cos\left(2\varepsilon \ln\frac{\Delta a}{4a}\right) + \sin(\theta-\phi)\sin\left(2\varepsilon \ln\frac{\Delta a}{4a}\right)\right] \tag{45}$$

where θ and ϕ are defined by

$$B = |B|e^{i\theta}$$

and

$$\phi = \tan^{-1}\frac{2\tan\psi_K}{1-\tan^2\psi_K}, \tag{46}$$

respectively. We introduce the Δa independent quantities $\bar{G}_I$ and $\bar{G}_{II}$ by extracting the magnitude of the oscillation terms in eqns (44)–(45) and neglecting the Δa terms in C for $\Delta a \ll 1$. Thus,

$$\bar{G}_I = \frac{1}{2}G + \frac{C|B|G}{D}[\cos(\theta-\phi)+\sin(\theta-\phi)]$$

$$= \frac{1}{2}G + \frac{\sqrt{2}C|B|G}{D}\cos\left(\theta-\phi-\frac{\pi}{4}\right) \tag{47}$$

$$\bar{G}_{II} = \frac{1}{2}G - \frac{C|B|G}{D}[\cos(\theta-\phi)+\sin(\theta-\phi)]$$

$$= \frac{1}{2}G - \frac{\sqrt{2}C|B|G}{D}\cos\left(\theta-\phi-\frac{\pi}{4}\right). \tag{48}$$

Solving eqns (44) and (45) for $(\theta-\phi)$ and substituting it into eqns (47) and (48), $\bar{G}_I$ and $\bar{G}_{II}$ can be expressed in terms of $\hat{G}_I$ and $\hat{G}_{II}$ as

$$\bar{G}_I = \frac{1}{2}G + \frac{\sqrt{2}C|B|G}{D}\cos\left(2\varepsilon\ln\frac{\Delta a}{4a} - \frac{\pi}{4} + \cos^{-1}\left(\frac{\hat{G}_I-\hat{G}_{II}}{2C|B|G}\right)\right) \tag{49}$$

$$\bar{G}_{II} = \frac{1}{2}G - \frac{\sqrt{2}C|B|G}{D}\cos\left(2\varepsilon\ln\frac{\Delta a}{4a} - \frac{\pi}{4} + \cos^{-1}\left(\frac{\hat{G}_I-\hat{G}_{II}}{2C|B|G}\right)\right). \tag{50}$$

Using the relations (49) and (50), $\bar{G}_I$ and $\bar{G}_{II}$ can be obtained through the calculation of $\hat{G}_I$ and $\hat{G}_{II}$ by the crack closure method. Meanwhile, the mode mixity can also be unambiguously represented by

$$\psi_{\bar{G}} = \tan^{-1}\left(\frac{\bar{G}_{II}}{\bar{G}_I}\right). \tag{51}$$

The mode mixity quantities ψ_K and $\psi_{\bar{G}}$ are related by

$$\tan\psi_{\bar{G}} = \frac{D-2\sqrt{2}C|B|\cos(\theta-\phi-\pi/4)}{D+2\sqrt{2}C|B|\cos(\theta-\phi-\pi/4)}. \tag{52}$$

Note that, in (52), ϕ is a function of ψ_K. Hence, the fracture criteria (41) and (42) can be expressed alternatively in terms of G and $\psi_{\bar{G}}$, or $\bar{G}_I$ and $\bar{G}_{II}$.

6. NUMERICAL RESULTS

By use of eqns (35) and (36), the stress intensity factors K_I and K_{II} can be obtained from $\hat{G}_I$ and $\hat{G}_{II}$ which can be calculated using finite elements with the aid of the crack closure method. The following numerical examples are selected to evaluate the accuracy of this approach. The present finite element calculations were carried out with the ABAQUS code. The eight-node isoparametric element was used for the analysis. The modified crack-closure method, based on the nodal forces and displacements, was used to compute the finite extension strain energy release rates $\hat{G}_I$ and $\hat{G}_{II}$.

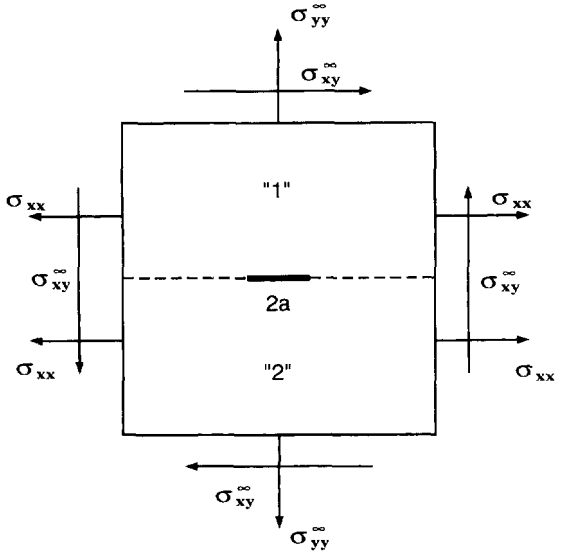

Fig. 2. An infinite bimaterial panel with a center crack under combined loading.

Table 2. Stress intensity factors for 100×100 plane stress panel subject to tensile and shear loading

		K_I			K_{II}		
E_1/E_2	$\sigma^{\infty}_{xy}/\sigma^{\infty}_{yy}$	Exact	Energy method	Error (%)	Exact	Energy method	Error (%)
10	0	1.6982	1.6976	0.04	−0.3185	−0.3195	0.30
	0.5	1.8575	1.8565	0.05	0.5306	0.5319	0.25
	1.0	2.0167	2.0175	0.04	1.3797	1.3771	0.19
100	0	1.6649	1.6642	0.04	−0.3790	−0.3793	0.08
	0.5	1.8544	1.8530	0.07	0.4535	0.4564	0.66
	1.0	2.0439	2.0456	0.09	1.2859	1.2815	0.34

The first example considered here is a finite center crack between two dissimilar isotropic materials in an infinite panel subject to both remotely uniform normal and shear stresses as shown in Fig. 2. For combined tensile and shear loading, the complete panel is considered. The size of the panel is 100×100 length unit with a finite crack of 2 length unit ($a = 1$); $\Delta a/a$ is chosen to be 0.01. The ratios of elastic moduli of the two materials considered in the analysis are $\nu_1/\nu_2 = 1$ and $E_1/E_2 = 10$ and 100. A state of plane stress is assumed. Comparison between the present calculations from the energy method and the analytical solution for a bimaterial medium derived by Rice and Sih (1965) is shown in Table 2. It is found that for K_I the average error is less than 0.1 and 0.6% for K_{II}. The relatively higher error for K_{II} is believed to be purely numerical resulting from a small $\hat{G}_{II}$ value. The corresponding strain energy release rates $\hat{G}_I$ and $\hat{G}_{II}$ obtained from the present calculation and the analytical solutions in (31) and (32) are shown in Table 3. It is also

Table 3. Strain energy release rates for 100×100 plane stress panel subject to tensile and shear loading

		$\hat{G}_I$			$\hat{G}_{II}$			
E_1/E_2	$\sigma^{\infty}_{xy}/\sigma^{\infty}_{yy}$	Exact eqn (31)	F.E.M. present	Error (%)	Exact eqn (32)	F.E.M. present	Error (%)	G error (%)
10	0	12.244	12.246	0.03	4.176	4.165	0.28	0.05
	0.5	5.982	5.963	0.31	14.543	14.550	0.05	0.06
	1.0	1.808	1.824	0.91	31.032	30.994	0.12	0.06
100	0	94.147	94.120	0.03	53.084	53.088	0.14	0.07
	0.5	35.042	34.766	0.79	148.99	149.15	0.10	0.07
	1.0	2.479	2.637	6.36	291.98	291.62	0.12	0.07

Table 4. Relative error of stress intensity factors obtained using displacement ratio method for $E_1/E_2 = 100$ and $\sigma_{xy}^{\infty}/\sigma_{xy}^{c} = 1.0$

Element number	First	Second	Third	Fourth	Fifth
x/a	0.01	0.02	0.03	0.04	0.05
Error for K_I(%)	2.72	0.67	0.37	0.24	0.13
Error for K_{II}(%)	6.46	1.54	0.82	0.48	0.19

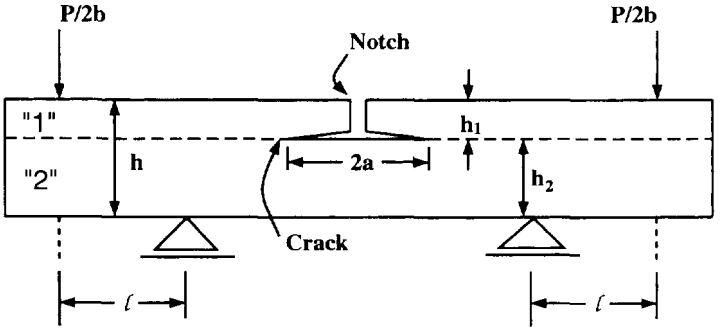

Fig. 3. A four-point bending beam with two symmetrical interface cracks.

observed that errors in the finite extension strain energy release rates are below 1%, except for very strong mismatches in elastic constants coupled with large shear loading. However, as seen from Tables 2 and 3, the large error in one of the strain energy release rates does not affect the high precision in K_I and K_{II}.

The displacement ratio method was also used to calculate the stress intensity factors for the above example. Crack surface displacements at various locations were taken to compute the displacement ratios. It is shown in Table 4 that errors for both K_I and K_{II} are less than 1% if the nodal displacements are taken at least two elements away from the crack tip.

The second example is a prenotched bimaterial beam in flexure shown in Fig. 3 originally considered by Matos *et al.* (1988) and by Suo and Hutchinson (1990) based on a beam model. Following the convention in Matos *et al.* (1988), the height h of the beam is chosen as the characteristic specimen dimension. In Tables 5–7, the stress intensity factors

Table 5. Comparison of normalized total strain energy release rate and stress intensity factors for a prenotched bimaterial beam in flexture with different E_1/E_2 ratios, $\nu_1 = \nu_2 = 0.3$, $a/l = 0.625$ and $h_1/a = 2.5$

	G^*		K_I^*		K_I^*	
E_2/E_1	Matos *et al.*	Present	Matos *et al.*	Present	Matos *et al.*	Present
1	10.4700	10.5027	2.4498	2.4496	2.1196	2.1219
10	6.4626	6.5094	0.7662	0.7614	0.8115	0.8198

$G^* = Gb^2h^3E_2/P^2l^2(1-\nu_2^2)$.
$K^* = K\cdot(h/2a)^{\alpha}bh^{3/2}\cosh(\pi\varepsilon)/Pl$.

Table 6. Comparison of normalized total strain energy release rate and stress intensity factors for different material mismatches in a prenotched bimaterial beam in flexture with $a/l = 0.625$, $h_1/a = 5$

		G^*		K_I^*		K_{II}^*	
α	β	Suo *et al.*	Present	Suo *et al.*	Present	Suo *et al.*	Present
0	0	10.5000	10.5027	2.4497	2.4496	2.1210	2.1218
−0.8	−0.2	6.8077	6.8091	0.8429	0.8412	0.8413	0.8432

$\alpha = (\mu_2(\kappa_1+1)-\mu_1(\kappa_2+1))/(\mu_2(\kappa_1+1)+\mu_1(\kappa_2+1))$.
$G^* = Gb^2h^3E_2/P^2l^2(1-\nu_2^2)$.
$K^* = K\cdot(h/2a)^{\alpha}bh^{3/2}\cosh(\pi\varepsilon)/Pl$.

Table 7. Normalized total strain energy release rate and stress intensity factors for a double cantilever beam with different E_1/E_2 ratios, $\nu_1 = \nu_2 = 0.3$, $a = l = 10$ and $h = 2$

		Energy method		Displacement ratio method	
E_2/E_1	G^*	K_I^*	K_{II}^*	K_I^*	K_{II}^*
1	7.7233	2.7791	0.0	2.7791	0.0
50	182.96	2.6002	−0.9995	2.5991	−1.0021
100	360.77	2.5822	−1.0414	2.5804	−1.0458

$G^* = Gb^2h^3E_2/P^2l^2(1-\nu_2^2)$.
$K^* = K\cdot(h/2a)^{\omega}bh^{3/2}\cosh(\pi\varepsilon)Pl$.

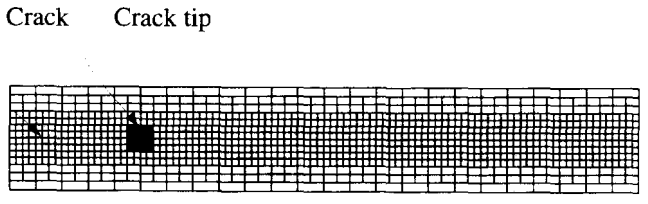

Fig. 4. Finite element mesh for right half of a bimaterial beam.

are also normalized by $Pl/bh^{3/2}$, and the strain energy release rates by $P^2l^2(1-\nu_2^2)/b^2h^3E_2$ where P is the applied load, l is the spacing between the inner and outer loading points, b is the width of the beam and E_1 the elastic modulus of the top layer. The plane strain condition is assumed.

Due to geometric and elastic symmetries with respect to its midsection, only the right half of the beam is modeled for the analysis. The finite element mesh used is shown in Fig. 4. The size of the smallest element of the crack tip is 0.01 length unit, and the inner loading point is at $a/l = 1.5$ for all the cases. From Table 5 we can see that the differences between the results of Matos *et al.* (1988) and present analysis based on the energy method are less than 1%. The comparison between the solution by Suo and Hutchinson (1990) and present results is presented in Table 6. Overall, it is seen that the results from the present analysis based on the energy method are in excellent agreement with those from the previous methods.

The last example is a double cantilever beam subject to a pair of opposite point loads as shown in Fig. 5. The same finite element mesh as in Fig. 4 was adopted for the analysis. The results for Gs and Ks based on the energy method and the displacement ratio method are listed in Table 7 for three different elastic mismatches. It is seen that the differences between these two methods are very small (within 0.5%). Also interesting to note is that

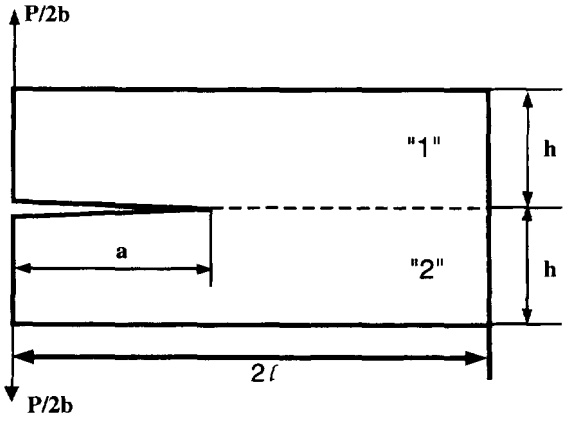

Fig. 5. A bimaterial double cantilever beam.

substantial shear mode (K_{II}) is induced by mode I type of loading if elastic material mismatches are large.

7. CONCLUSION

From the comparison of the near tip stress fields for interfacial cracks in bimaterial media obtained from the contact model and the oscillatory model, we conclude that, except for the extremely small contact zone near the crack tip, the two solutions are basically identical. This justifies the use of the oscillatory model for the fracture analysis of interfacial cracks for a small contact zone. The Mode I and Mode II strain energy release rates $\hat{G}_I$ and $\hat{G}_{II}$ for finite crack extensions can easily be obtained from the finite element analysis using the crack closure method. The stress intensity factors derived from $\hat{G}_I$ and $\hat{G}_{II}$ are very accurate. It was also shown that the ratio of stress intensity factors can also be obtained very accurately from the crack surface displacement ratio. This ratio in conjunction with the total strain energy release rate can be used to evaluate the stress intensity factors with excellent results. The non-oscillatory quantities $\bar{G}_I$ and $\bar{G}_{II}$ derived from $\hat{G}_I$ and $\hat{G}_{II}$ can be used to give an alternative expression for the interfacial crack mode mixity. Thus, the fracture criterion can be given in terms of the total strain energy release rate G and the ratio $\bar{G}_{II}/\bar{G}_I$ with no need to calculate the stress intensity factors.

Acknowledgements—This work was supported in part by a Purdue Research Foundation grant and in part by the Office of Naval Research grant no. N00014-90-J-1666 for which Dr Y.D.S. Rajapakse was the grant monitor.

REFERENCES

Bui, H. D. (1994). *Inverse Problem in the Mechanics of Materials: An Introduction*. CRC Press, Boca Raton, Ann Arbor, London.

Comninou, M. (1977). The interface crack. *Journal of Applied Mechanics* **44,** 631–636.

Comninou, M. (1978). The interface crack in a shear field. *Journal of Applied Mechanics* **45,** 287–290.

Comninou, M. and Schmueser, D. (1979). The interface crack in a combined tension-compression and shear field. *Journal of Applied Mechanics* **46,** 345–348.

England, A. H. (1965). A crack between dissimilar media. *Journal of Applied Mechanics* **32,** 400–402.

Gautsen, A. K. (1993). The interface crack under combined loading: an eigenvalue problem for the gap. *International Journal of Fracture* **60,** 349–361.

Gautsen, A. K. and Dundurs, J. (1987). The interface crack in a tension field. *Journal of Applied Mechanics* **54,** 93–98.

Gautsen, A. K. and Dundurs, J. (1988). The interface crack under combined loading. *Journal of Applied Mechanics* **55,** 580–586.

Hutchinson, J. W. (1990). Mixed mode fracture mechanics of interfaces, metal–ceramic interface. *ActaScripta Metallurgica* **4,** 295–306.

Hutchinson, J. W., Mear, M. and Rice, J. R. (1987). Crack paralleling an interface between dissimilar materials. *Journal of Applied Mechanics* **54,** 828–832.

Jih, C. J. and Sun, C. T. (1990). Evaluation of a finite element based crack-closure method for calculating static and dynamic strain energy release rates. *Engineering Fracture Mechanics* **37,** 313–322.

Lin, K. Y. and Mar, J. W. (1976). Finite element analysis of stress intensity factors for cracks at a bi-material interface. *International Journal of Fracture* **12,** 521–531.

Malysev, B. M. and Salganik, R. L. (1965). The strength of adhesive joints using the theory of cracks. *International Journal of Fracture* **1,** 114–127.

Matos, P. P. L., McMeeking, R. M., Charalamibides, P. G. and Drory, D. (1989). A method for calculating stress intensities in bimaterial fracture. *International Journal of Fracture* **40,** 235–254.

Raju, I. S., Crews, Jr, J. H. and Aminpour, M. A. (1988). Convergence of strain energy release rate components for edge-delaminated composite laminates. *Engineering Fracture Mechanics* **30,** 383–396.

Rice, J. R. (1988). Elastic fracture mechanics concepts for interfacial cracks. *Journal of Applied Mechanics* **55,** 98–103.

Rice, J. R. and Sih, G. C. (1965). Plane problems of cracks in dissimilar media. *Journal of Applied Mechanics* **32,** 418–423.

Rybicki, E. F. and Kanninen, M. F. (1977). A finite element calculation of stress intensity factors by a modified crack closure integral. *Engineering Fracture Mechanics* **9,** 931–938.

Sun, C. T. and Jih, C. J. (1987). On strain energy release rate for interfacial cracks in bimaterial media. *Engineering Fracture Mechanics* **28,** 13–20.

Suo, Z. and Hutchinson, J. W. (1990). Interface crack between two elastic layers. *International Journal of Fracture* **43,** 1–18.

Williams, M. L. (1959). The stresses around a fault or crack in dissimilar media. *Bulletin of the Seismolology Society of America* **49,** 199–204.

APPENDIX

The parameters $\hat{s}_1$, $\hat{s}_3$, w_1 and w_3 in eqns (11) and (12) are given by Gautsen and Dundurs (1987) and listed here as

$$\hat{s}_1(w) = 2\sin[\beta_0(\pi - w)/(2\lambda)]E_0(w)/[1 - E_0(w)]$$

$$\hat{s}_3(w) = 2E_0(w)\{\cos[\beta_0(\pi - w)/(2\lambda)] - E_0^{-1/2}(w)\}/[1 - E_0(w)]$$

where

$$E_0(w) = \exp[-\pi(\pi - w)/\lambda]$$

$$w = \lambda q_0(x)$$

$$w_2 = \beta_0 q_0(x)/2$$

$$q_0(x) = 2/\pi \log\{2[x + (x^2 + k^2)^{1/2}]\}/\{k[1 + (x^2 + 1)^{1/2}]\} + o(k^2 \log(k))$$

$$\lambda = \pi\beta_0/[\pi + 2\tan^{-1}(\beta_0/\pi)]$$

$$k^2 = 16\exp\{-(\pi^2/\beta_0) - [(2/\pi)\tan^{-1}(\beta_0/\pi) + 1]\}$$